

Low-temperature thermometry enhanced by strong coupling

Luis A. Correa,^{1,2} Martí Perarnau-Llobet,^{3,4} Karen V. Hovhannisyanyan,³
Senaida Hernández-Santana,³ Mohammad Mehboudi,² and Anna Sanpera^{2,5}

¹*School of Mathematical Sciences and Centre for the Mathematics and Theoretical Physics of Quantum Non-Equilibrium Systems, The University of Nottingham, University Park, Nottingham NG7 2RD, United Kingdom**

²*Departament de Física, Universitat Autònoma de Barcelona, 08193 Bellaterra, Spain*

³*Institut de Ciències Fotòniques (ICFO), The Barcelona Institute of Science and Technology, 08860 Castelldefels (Barcelona), Spain*

⁴*Max-Planck-Institut für Quantenoptik, Hans-Kopfermann-Str. 1, D-85748 Garching, Germany*

⁵*Institució Catalana de Recerca i Estudis Avançats (ICREA), 08011 Barcelona, Spain*

(Dated: June 4, 2022)

We consider the problem of estimating the temperature T of a very cold equilibrium sample with an individual quantum probe. In particular, T is inferred from measurements performed on a single quantum harmonic probe strongly coupled to the sample under investigation. Due to the non-perturbative probe-sample interaction the stationary state of the former will not be thermal, in general. This turns out to be potentially advantageous for measuring low temperatures, as we show that: (i) The thermometric precision at low T can be significantly enhanced by strengthening the probe-sampling coupling, (ii) the variance of a suitable quadrature of our single-mode thermometer can yield temperature estimates with nearly minimal statistical uncertainty, and (iii) the spectral density of the probe-sample coupling may be engineered to further improve thermometric performance. These observations may find applications in practical nanoscale thermometry at low temperatures—a regime which is particularly relevant to quantum technologies.

PACS numbers: 06.20.-f, 03.65.-w, 03.65.Yz, 07.20.Mc

The development of *nanoscale* temperature sensing techniques has attracted an increasing interest over the last few years [1] due to their potential applications to microelectronics [2–4], biochemistry, or even to disease diagnosis [5–8]. In particular, thermometer miniaturization may be taken to the extreme of devising individual *quantum* thermometers [6, 9–12]. The problem of measuring the temperature T of an equilibrium sample is most often tackled by thermally coupling it to a probe. After equilibration, one can estimate T by monitoring some temperature-dependent feature of the probe via a suitable measurement and data analysis scheme. Provided that the heat capacity of the probe is sufficiently low, one usually assumes that the back-action on the sample can be neglected, and that the probe ends up in a Gibbs state at the sample temperature.

Such a simple picture runs into trouble if the sample is *too cold*, especially when using an individual quantum thermometer: The seemingly natural assumption of the probe reaching equilibrium at the sample temperature might break down at low T . In this limit, the two parties can build up enough correlations to eventually keep the probe from thermalizing [13–16]. Furthermore, if the probe is *too small*, boundary effects become relevant and need to be taken into account to properly describe equilibration and thermalization [16–19].

One could still assume thermalization in the standard sense, owing to a vanishing probe-sample coupling. However, in this limit the ‘thermal sensitivity’ of the probe, which is proportional to its heat capacity [20–23], drops quickly as the temperature decreases [24]. As is shown in [25] and in Appendix A, this is an inherent problem of low-temperature thermometry. The main aim of this article is to show how to fight

such a fundamental limitation.

In particular, we extend quantum thermometry to the *strong coupling* regime, by adopting a fully rigorous description of the probe’s dynamics. We model the equilibrium sample as a structured bosonic reservoir [26, 27], and couple it to a single-mode quantum thermometer. We calculate the steady state of the probe exactly and show that its low-temperature thermal sensitivity is significantly enhanced by increasing the coupling strength. While strong dissipation is most often detrimental within quantum technologies, here we find that low temperature quantum thermometry is indeed boosted by strong dissipative interactions.

In order to quantify the maximum sensitivity attainable by our quantum thermometer, we make use of the quantum Fisher information (QFI) associated to temperature estimation \mathcal{F}_T [28, 29]. Essentially, \mathcal{F}_T sets a lower bound on the ‘error bars’ $\delta T \geq 1/\sqrt{M\mathcal{F}_T}$ of any estimate of the temperature of the sample processed from the outcomes of M measurements on the probe [30]. Although energy measurements are known to be optimal for thermometry with a probe in thermal equilibrium [31], we will see that these do not harness the potential improvement allowed by a strong probe-sample coupling.

It is important to stress that our results are not limited by any of the simplifying assumptions usually adopted when dealing with open quantum systems, such as the Born-Markov or secular approximations, nor they rely on perturbative expansions in the ‘dissipation strength’ [32]. Our only requirement is that probe and sample are initially uncorrelated.

We shall now motivate our analysis by illustrating the inherent difficulty of measuring low temperatures. Let us start by considering a quantum probe weakly coupled to a thermal sample, so that its steady state can be written as $\rho_T = e^{-\beta H_p}/\mathcal{Z}$, where H_p is the Hamiltonian of the probe and $1/\beta = T$ is the temperature of the sample (we will assume

* luis.correa@nottingham.ac.uk

$k_B = \hbar = 1$ throughout this article, and \mathcal{L} stands for the partition function). The quantum Fisher information for temperature \mathcal{F}_T can be formally defined as [28]

$$\mathcal{F}_T := -2 \lim_{\delta \rightarrow 0} \partial^2 \mathbb{F}(\rho_T, \rho_{T+\delta}) / \partial \delta^2. \quad (1)$$

Here, $\mathbb{F}(\rho, \sigma) := \left(\text{tr} \sqrt{\sqrt{\rho} \sigma \sqrt{\rho}} \right)^2$ stands for the Uhlmann fidelity between states ρ and σ [33, 34]. The Uhlmann fidelity relates to the Bures distance $d_B^2(\rho, \sigma) := 2(1 - \sqrt{\mathbb{F}(\rho, \sigma)})$ between ρ and σ [35, 36]. Intuitively, \mathcal{F}_T gauges the *distinguishability* of probes at infinitesimally close temperatures.

The QFI of our single-mode equilibrium thermometer evaluates to $\mathcal{F}_T^{(\text{eq})}(\omega) = \frac{\omega^2}{4T^4} \text{csch}^2\left(\frac{\omega}{2T}\right)$, which remains roughly constant and close to its maximum within a wide range of temperatures [31]. However, $\mathcal{F}_T^{(\text{eq})}(\omega)$ does decay exponentially at low T [37], which can be inferred by expanding it as $\mathcal{F}_T^{(\text{eq})}(\omega) = \frac{\omega^2}{2T^4} e^{-\omega/T} + \mathcal{O}(e^{-2\omega/T})$ for $T/\omega \rightarrow 0$. This is not specific to harmonic probes, but generally applicable to, e.g., optimized finite-dimensional equilibrium thermometers [31]. That is, even an estimate based on the most informative measurements on an optimized *equilibrium* probe has an exponentially vanishing precision at low T .

Interestingly, one can prove that the thermal sensitivity of any small fraction of a large many-body system in global thermal equilibrium is exponentially suppressed at low temperatures when away from criticality, and provided that the interactions are short-ranged (see Appendix A). Specifically,

$$\mathcal{F}_T \leq \mathcal{O}(1) (\Delta/T)^5 e^{-\Delta/T} \quad T/\Delta \ll 1, \quad (2)$$

where Δ bounds the minimum energy gap of the system from below. Importantly, Eq. (2) holds regardless of the interaction strengths, hence implying that low-temperature local quantum thermometry is, in general, *exponentially inefficient*. It is precisely this fundamental limitation which makes practical strategies to improve low-temperature sensitivity ever more relevant, even if these can not resolve the bad scaling of \mathcal{F}_T .

In what follows, we will show that the thermal sensitivity can indeed improve (at low enough T) as the probe-sample coupling is increased, and the correlations built up among the two eventually allow the probe to sense a ‘larger’ portion of the sample. Namely, we will find the exact (non-equilibrium) steady-state of a harmonic probe under arbitrarily strong dissipation into an equilibrium environment, to then compute its maximum thermal sensitivity. In order to describe the probe-sample interaction, we adopt the standard Caldeira-Leggett model [26, 38]. In this case, the Hamiltonian of the probe is just $H_p = \frac{1}{2} \omega_0^2 x^2 + \frac{1}{2} p^2$ (where the mass of the probe is $m = 1$), whereas the sample is described as an infinite collection of non-interacting bosonic modes $H_s = \sum_{\mu} \frac{1}{2} \omega_{\mu}^2 m_{\mu} x_{\mu}^2 + \frac{1}{2m_{\mu}} p_{\mu}^2$. The probe-sample coupling is realized by a linear term of the form $H_{p-s} = x \sum_{\mu} g_{\mu} x_{\mu}$. In order to compensate exactly for the ‘distortion’ caused on the probe by the coupling to the sample, one should replace ω_0^2 with $\omega_0^2 + \omega_R^2$ in H_p [26, 38], where the ‘renormalization frequency’ is $\omega_R^2 := \sum_{\mu} \frac{g_{\mu}^2}{m_{\mu} \omega_{\mu}^2}$ [39].

The coupling strengths between the probe and each of the sample modes are determined by the ‘spectral density’

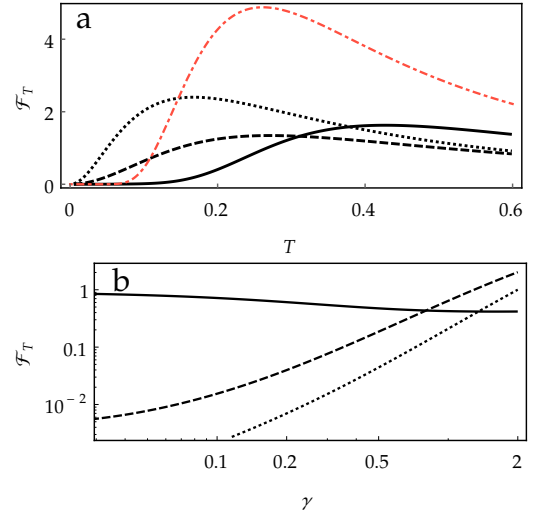


FIG. 1. (color online) (a) Quantum Fisher information \mathcal{F}_T vs. the sample temperature T for different dissipation strengths: (solid black) $\gamma = 0.1$, (dashed black) $\gamma = 1$, and (dotted black) $\gamma = 5$ ($\omega_0 = 1$). The sensitivity of a single-mode probe at thermal equilibrium (dot-dashed red) has been super-imposed for comparison. (b) Log-log plot of \mathcal{F}_T as a function of γ for (solid) $T = 1$, (dashed) $T = 0.1$, and (dotted) $T = 0.05$. In both cases we work in units of $\hbar = k_B = 1$. Here, $\omega_c = 100 \omega_0$.

$J(\omega) := \pi \sum_{\mu} \frac{g_{\mu}^2}{2m_{\mu} \omega_{\mu}} \delta(\omega - \omega_{\mu})$, which is given a phenomenological analytical form. To ensure convergence, one must set up a high-frequency cutoff in $J(\omega)$ [38]. In what follows, we shall work with an Ohmic spectral density with Lorentz-Drude cutoff $J(\omega) = 2\gamma \omega \omega_c^2 / (\omega^2 + \omega_c^2)$, which vanishes for $\omega \gg \omega_c$. Here, γ stands for the dissipation strength and carries the order of magnitude of the couplings g_{μ} [40].

The following equation of motion for $x(t)$ can be obtained from the Heisenberg equations for x , p , x_{μ} and p_{μ} :

$$\ddot{x}(t) + (\omega_0^2 + \omega_R^2)x(t) - x(t) * \chi(t) = F(t). \quad (3)$$

This is the quantum Langevin equation (QLE) [38, 41] for the probe. The first two terms in the left-hand side of Eq. (3) correspond to the coherent dynamics of a free harmonic oscillator of squared frequency $\omega_0^2 + \omega_R^2$ (the dots denote time derivative), while the incoherent superposition of all environmental modes, encompassed in $F(t)$, plays the role of a stochastic driving force (see Appendix B). Finally, the convolution $x(t) * \chi(t) := \int_{-\infty}^{\infty} ds \chi(t-s)x(s)$ brings memory effects into the dissipative dynamics. This is given by $\chi(t) = \frac{2}{\pi} \Theta(t) \int_0^{\infty} d\omega J(\omega) \sin \omega t$, where $\Theta(t)$ stands for the Heaviside step function, which is needed to ensure causality.

It is important to remark that Eq. (3) is *exact*. As already advanced, the only assumption that we make is that probe and sample start uncorrelated at $t_0 \rightarrow -\infty$, i.e. in $\rho \otimes \sigma_T$, where σ_T is the Gibbs state of the sample at temperature T . The initial state of the probe ρ is arbitrary. However, since the Hamiltonian H is overall bilinear in positions and momenta, its stationary state is Gaussian, and thus, completely determined by its second-order moments $\sigma_{ij}(t', t'') := \frac{1}{2} \langle \{R_i(t'), R_j(t'')\} \rangle$,

where $R = (x, p)$ [41]. The notation $\langle \dots \rangle$ stands here for average on the initial state and $\{ \dots \}$ denotes anti-commutator.

One may now take the Fourier transform ($\tilde{f}(\omega) := \int_{-\infty}^{\infty} dt f(t) e^{i\omega t}$) in Eq. (3), and solve for $\tilde{x}(\omega)$, which yields

$$\tilde{x}(\omega) = [\omega_0^2 + \omega_R^2 - \omega^2 - \tilde{\chi}(\omega)]^{-1} \tilde{F}(\omega) := \alpha(\omega)^{-1} \tilde{F}(\omega). \quad (4)$$

The position correlator $\sigma_{11}(t', t'')$ can be thus cast as

$$\sigma_{11} = \iint_{-\infty}^{\infty} \frac{d\omega' d\omega''}{8\pi^2} e^{-i(\omega't' + \omega''t'')} \langle \{ \tilde{x}(\omega'), \tilde{x}(\omega'') \} \rangle, \quad (5)$$

whereas σ_{22} may be calculated similarly by noticing that $\langle \{ \tilde{p}(\omega'), \tilde{p}(\omega'') \} \rangle = -\omega' \omega'' \langle \{ \tilde{x}(\omega'), \tilde{x}(\omega'') \} \rangle$. The two remaining correlators simply vanish ($\sigma_{12} = \sigma_{21} = 0$) (see Appendix E).

Hence, in light of Eqs. (4) and (5), all we need to know is the power spectrum of the noise $\langle \{ \tilde{F}(\omega'), \tilde{F}(\omega'') \} \rangle$ and the Fourier transform of the dissipation kernel $\tilde{\chi}(\omega)$. Since the sample was prepared in a Gibbs state, one can show that the noise is connected to the dissipation kernel through the following fluctuation-dissipation relation (see Appendix C 1)

$$\langle \{ \tilde{F}(\omega'), \tilde{F}(\omega'') \} \rangle = 4\pi \delta(\omega' + \omega'') \coth\left(\frac{\omega'}{2T}\right) \text{Im} \tilde{\chi}(\omega'). \quad (6)$$

For our specific choice of spectral density $J(\omega)$, $\tilde{\chi}(\omega)$ evaluates to $\tilde{\chi}(\omega) = 2\gamma\omega_c^2/(\omega_c - i\omega)$.

Putting together the pieces from the above paragraphs, we can compute the steady-state covariances $\sigma_{ij}(0, 0)$ [42, 43] (recall that $t_0 \rightarrow -\infty$). These may be collected into the 2×2 covariance matrix σ , which provides a full description of the (Gaussian) non-equilibrium asymptotic state of our single-mode probe [44]. We can now calculate \mathcal{F}_T from Eq. (1), using the fact that the Uhlmann fidelity between two single-mode Gaussian states with covariance matrices σ_1 and σ_2 is given by $\mathbb{F}(\sigma_1, \sigma_2) = 2 \left(\sqrt{\Delta + \Lambda} - \sqrt{\Lambda} \right)^{-1}$, where $\Delta := 4 \det(\sigma_1 + \sigma_2)$ and $\Lambda := (4 \det \sigma_1 - 1)(4 \det \sigma_2 - 1)$ [45].

In Fig. 1(a) we plot the thermal sensitivity \mathcal{F}_T of a harmonic probe as a function of the sample temperature, for several (large) values of the dissipation strength γ . When comparing it with the sensitivity of an equilibrium mode, we can see that, even though the overall maximum attainable sensitivity may be deterred by a stronger probe-sample coupling, the low-temperature QFI does increase significantly as the dissipation strength grows. This is further illustrated in Fig. 1(b), where we plot \mathcal{F}_T as a function of γ for different temperatures: As shown in the figure, if the sample is cold enough, the sensitivity of the probe increases *monotonically* with the dissipation strength. Hence, the probe-sample coupling can be thought-of as a relevant control parameter in practical low-temperature quantum thermometry. This is our main result.

Thus far, we have shown how strong coupling may improve the ultimate bounds on thermometric precision at low temperatures. However, we have not yet discussed how to saturate those bounds in practice. We therefore need to find observables capable of producing temperature estimates that approach closely the precision bound set by the QFI.

In general, a temperature estimate based on M measurements of some observable O on the steady state of the

probe has uncertainty $\delta T \geq 1/\sqrt{M \mathcal{F}_T(O)}$, where $\mathcal{F}_T(O)$ stands for the ‘classical Fisher information’ of O [29]. This may be lower-bounded by the ‘thermal sensitivity’ $F_T(O) := |\partial_T \langle O \rangle|^2 / (\Delta O)^2 \leq \mathcal{F}_T(O) \leq \mathcal{F}_T \equiv \sup_O \mathcal{F}_T(O)$ [28]. Here, $\Delta O := \sqrt{\langle O^2 \rangle - \langle O \rangle^2}$ denotes standard deviation and all averages are taken with respect to the stationary state of the probe.

The observable for which $F_T(O)$ is maximized commutes with the so-called ‘symmetric logarithmic derivative’ (SLD) L , which satisfies $\partial_T \rho = \frac{1}{2}(L\rho + \rho L)$. For instance, in the case of an equilibrium probe, i.e. $\rho_T \propto \exp(-H_p/T)$, one has $[L, H_p] = 0$. Consequently, a complete projective measurement on the energy measurements renders the best temperature estimate. However, as shown in Fig. 2, when the strength of the interaction with the sample increases, energy measurements become less and less informative about the temperature of the sample: the larger the dissipation strength γ , the smaller $F_T(H_p)/\mathcal{F}_T$. Temperature estimates based on energy measurements seem thus incapable of exploiting the extra low-temperature sensitivity enabled by the strong dissipation.

In searching for a more suitable measurement scheme, one can look at the SLD: Since ρ_T is an undisplaced Gaussian (see Appendix C), L will be a quadratic form of x^2 and p^2 [46]. Due to our choice for the probe-sample coupling ($x \sum_{\mu} g_{\mu} x_{\mu}$), the steady state ρ_T becomes squeezed in the position quadrature when the temperature is low enough and the dissipation rate is sufficiently large. Interestingly, we observe that $\langle x^2 \rangle$ is much more sensitive to temperature changes in this regime than $\langle p^2 \rangle$. We thus take $O = x^2$ as an ansatz for a quasi-optimal temperature estimator. $F_T(x^2)$ is also plotted in Fig. 2, where we can see how it does approach closely the ultimate bound \mathcal{F}_T as γ grows. Note that the quadratures of e.g. a single trapped ion are either directly measurable [47] or accessible via state tomography [48, 49]. Measuring the variance

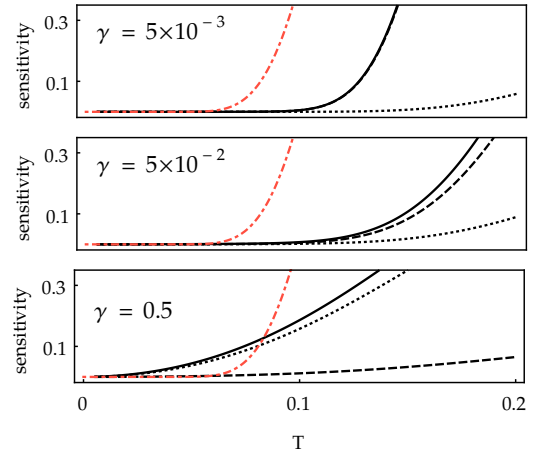


FIG. 2. (color online) Comparison of (solid black) the maximum thermal sensitivity \mathcal{F}_T of the non-equilibrium probe, (dashed black) the sub-optimal sensitivity of the average energy $F_T(H_p)$, (dotted black) the sensitivity of the position covariance $F_T(x^2)$, for different values of the dissipation strength: $\gamma = 5 \times 10^{-3}$, $\gamma = 5 \times 10^{-2}$, and $\gamma = 0.5$. Again, the thermal sensitivity of the corresponding equilibrium state has been added for comparison (dot-dashed red), and $\omega_c = 100 \omega_0$.

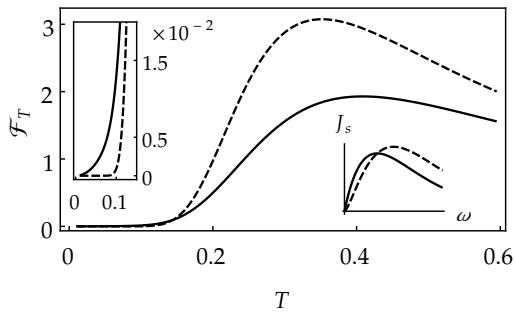


FIG. 3. Quantum Fisher information \mathcal{F}_T as a function of temperature for (solid) Ohmic and (dashed) super-Ohmic spectral density $J_s(\omega)$ with exponential high-frequency cutoff. (top left) Zoom into the low-temperature region of the main plot. (bottom right) comparison of the (solid) Ohmic and (dashed) super-Ohmic spectral densities. In this plots $\omega_0 = 1$, $\gamma = 0.1$, and $\omega_c = 100\omega_0$.

of the most relevant quadrature of a harmonic thermometer is therefore a practical prescription capable of exploiting the thermometric advantage provided by strong dissipation at low temperatures.

To conclude, we shall give an intuition about the origin of the observed dissipation-driven enhancement. To that end, let us consider not just the marginal of the probe but the global state of probe *and* sample. For simplicity we can model them as a finite N -mode ‘star system’, comprised of a central harmonic oscillator (playing the role of the probe), linearly coupled to $N - 1$ independent peripheral oscillators with arbitrary frequencies (representing the sample). Let us further prepare the N -mode composite in a Gibbs state at the sample temperature T . Indeed, when such linear system is at global thermal equilibrium, and provided that the number of modes N is large enough, the marginal of the central oscillator approximates well the *actual* steady state of the probe, which we have just calculated exactly [14].

It is easy to see that, whatever the distribution of the couplings, the frequencies of the lowermost normal modes of the global star system always *decrease monotonically* as the overall magnitude of the coupling strengths increases (see Appendix F). If the temperature T was so low that not even the first harmonic could get thermally populated, the sensitivity of the entire system and, by extension, also that of the central probe, would vanish. However, one could populate the first few normal modes by strengthening the couplings, as their frequencies would then decrease. It is this effect which ultimately enables temperature sensing at low T . The magnitude of the enhancement is dictated by the specific frequency distribution of the probe-sample couplings which, in turn, determines the spectrum of the normal modes of the global system (see Appendices F and A).

From the above reasoning it follows that the *shape* of the

spectral density $J(\omega)$ could, in principle, be tailored to render more precise low-temperature probes. To see that this is indeed the case, we shall adopt a generic spectral density of the form $J_s(\omega) := \frac{\pi}{2} \gamma \omega^s \omega_c^{1-s} e^{-\omega/\omega_c}$, i.e. with an exponential high-frequency cutoff. We can thus compare the performance of a single-mode thermometer coupled to the sample through an Ohmic ($s = 1$) and a super-Ohmic ($s > 1$) spectral density, e.g. at fixed γ . For this purpose, we resort again to Eqs. (4)–(6), leading to the exact Gaussian marginal of the probe. Importantly, the dissipation kernel $\tilde{\chi}(\omega)$ needs to be re-calculated due to the change in spectral density (see Appendix D and [43]). Note as well that now $\omega_R = \gamma \omega_c \Gamma(s)$, where $\Gamma(z) := \int_0^\infty dt t^{z-1} e^{-t}$ is Euler’s Gamma function. The results are illustrated in Fig. 3: As we can see, a super-Ohmic spectral density (in our case, with $s = 2$) may allow for a large improvement over an Ohmic one, in terms of maximum achievable thermal sensitivity (also compare with Fig. 1). On the contrary, when it comes to thermometric precision at low temperatures, the Ohmic spectral density offers a clear advantage. As a final remark, we note that, since the equilibrium state of the probe corresponds to the marginal of a global thermal state [14], we can think of our results as an instance of thermometry on a macroscopic sample through local measurements, as studied in [25].

The aim of this study has been threefold: (i) We have shown that the thermal sensitivity of a single-mode bosonic probe can be boosted by increasing the strength of its dissipative coupling to the sample under study, (ii) we have provided a concrete and feasible measurement scheme capable of producing nearly optimal temperature estimates in the relevant regime and, finally, (iii) we have suggested that the spectral density of the probe-sample coupling can be set to play an active role in enhanced low-temperature quantum thermometry. Our results may be particularly relevant to practical nanoscale thermometry, taking into account the marked decay of the thermometric precision at low temperatures. It is worth emphasizing that all our results are exact, irrespective of the relative ordering of the various time scales involved in the problem. In particular, observation (iii) calls for a more in-depth analysis of the potential role of reservoir engineering techniques [50, 51] or even dynamical control [52] in enhanced low-temperature quantum thermometry and will be the subject of further investigation.

Acknowledgements.– We thank Antonio Acín, Antonio A. Valido, Emili Bagan and Alex Monras for fruitful discussions. We acknowledge funding from the European Research Council (ERC) Starting Grant QCCOP (Grant No. 637352), the EU Collaborative Project TherMiQ (Grant Agreement 618074), the Spanish MINECO (Project No. FIS2013-40627-P, FQUS FIS2013-46768-P, and Severo Ochoa SEV-2015-0522), the Generalitat de Catalunya (CIRIT Project No. 2014 SGR 966 and SGR 875), a CELLEX-ICFO-MPQ Research Fellowships, and the COST Action MP1209.

[1] L. Carlos and F. Palacio, *Thermometry at the Nanoscale: Techniques and Selected Applications*, Vol. 38 (Royal Society of

Chemistry, 2015).

- [2] C. C. Williams and H. K. Wickramasinghe, “Scanning thermal profiler,” *Appl. Phys. Lett.* **49**, 1587–1589 (1986).
- [3] L. Aigouy, G. Tessier, M. Mortier, and B. Charlot, “Scanning thermal imaging of microelectronic circuits with a fluorescent nanoprobe,” *Appl. Phys. Lett.* **87**, 184105 (2005).
- [4] S. Lefèvre and S. Volz, “ 3ω -scanning thermal microscope,” *Rev. Sci. Instrum.* **76**, 033701 (2005).
- [5] B. Klinkert and F. Narberhaus, “Microbial thermosensors,” *Cell. Mol. Life Sci.* **66**, 2661–2676 (2009).
- [6] G. Kucsko, P. C. Maurer, N. Y. Yao, M. Kubo, H. J. Noh, P. K. Lo, H. Park, and M. D. Lukin, “Nanometre-scale thermometry in a living cell,” *Nature* **500**, 54–58 (2013).
- [7] R. Schirhagl, K. Chang, M. Loretz, and C. L. Degen, “Nitrogen-vacancy centers in diamond: nanoscale sensors for physics and biology,” *Annu. Rev. Phys. Chem.* **65**, 83–105 (2014).
- [8] B. Somogyi and A. Gali, “Computational design of in vivo biomarkers,” *J. Phys. Condens. Matter* **26**, 143202 (2014).
- [9] F. Seilmeier, M. Hauck, E. Schubert, G. J. Schinner, S. E. Beavan, and A. Högele, “Optical Thermometry of an Electron Reservoir Coupled to a Single Quantum Dot in the Millikelvin Range,” *Phys. Rev. Applied* **2**, 024002 (2014).
- [10] F. Haupt, A. Imamoglu, and M. Kroner, “Single Quantum Dot as an Optical Thermometer for Millikelvin Temperatures,” *Phys. Rev. Applied* **2**, 024001 (2014).
- [11] P. Neumann, I. Jakobi, F. Dolde, C. Burk, R. Reuter, G. Waldherr, J. Honert, T. Wolf, A. Brunner, J. H. Shim, *et al.*, “High-precision nanoscale temperature sensing using single defects in diamond,” *Nano Lett.* **13**, 2738–2742 (2013).
- [12] T. H. Johnson, F. Cosco, M. T. Mitchison, D. Jaksch, and S. R. Clark, “Thermometry of ultracold atoms via nonequilibrium work distributions,” *Phys. Rev. A* **93**, 053619 (2016).
- [13] Th. M. Nieuwenhuizen and A. E. Allahverdyan, “Statistical thermodynamics of quantum Brownian motion: Construction of perpetual mobile of the second kind,” *Phys. Rev. E* **66**, 036102 (2002).
- [14] Y. Subaşı, C. H. Fleming, J. M. Taylor, and B. L. Hu, “Equilibrium states of open quantum systems in the strong coupling regime,” *Phys. Rev. E* **86**, 061132 (2012).
- [15] M. Ludwig, K. Hammerer, and F. Marquardt, “Creation and destruction of entanglement by a nonequilibrium environment,” *Phys. Rev. A* **82**, 012333 (2010).
- [16] C. Gogolin and J. Eisert, “Equilibration, thermalisation, and the emergence of statistical mechanics in closed quantum systems,” *Reports on Progress in Physics* **79**, 056001 (2016).
- [17] A. Ferraro, A. García-Saez, and A. Acín, “Intensive temperature and quantum correlations for refined quantum measurements,” *EPL (Europhysics Letters)* **98**, 10009 (2012).
- [18] M. Kliesch, C. Gogolin, M. J. Kastoryano, A. Riera, and J. Eisert, “Locality of Temperature,” *Phys. Rev. X* **4**, 031019 (2014).
- [19] S. Hernández-Santana, A. Riera, K. V. Hovhannisyán, M. Perarnau-Llobet, L. Tagliacozzo, and A. Acín, “Locality of temperature in spin chains,” *New J. Phys.* **17**, 085007 (2015).
- [20] L. D. Landau and E. M. Lifshitz, *Statistical Physics*, 1st ed. (Clarendon, Oxford, 1938).
- [21] B. B. Mandelbrot, “An outline of a purely phenomenological theory of statistical thermodynamics: I. Canonical ensembles,” *IRE Trans. Inf. Theory* **2**, 190–203 (1956).
- [22] B. B. Mandelbrot, “Temperature fluctuation: a well-defined and unavoidable notion,” *Physics Today* **42**, 71 (1989).
- [23] J. Uffink and J. van Lith, “Thermodynamic Uncertainty Relations,” *Found. Phys.* **29**, 655–692 (1999).
- [24] P. Debye, “Zur theorie der spezifischen wärmen,” *Ann. Phys. (Berlin)* **344**, 789–839 (1912).
- [25] A. De Pasquale, D. Rossini, R. Fazio, and V. Giovannetti, “Local quantum thermal susceptibility,” *Nat. Commun.* **7**, 12782 (2016).
- [26] A. O. Caldeira and A. J. Leggett, “Path integral approach to quantum Brownian motion,” *Phys. A* **121**, 587–616 (1983).
- [27] P. S. Riseborough, P. Hänggi, and U. Weiss, “Exact results for a damped quantum-mechanical harmonic oscillator,” *Phys. Rev. A* **31**, 471 (1985).
- [28] S. L. Braunstein and C. M. Caves, “Statistical distance and the geometry of quantum states,” *Phys. Rev. Lett.* **72**, 3439–3443 (1994).
- [29] O. E. Barndorff-Nielsen and R. D. Gill, “Fisher information in quantum statistics,” *J. Phys. A* **33**, 4481 (2000).
- [30] H. Cramér, *Mathematical methods of statistics*, Vol. 9 (Princeton university press, 1999).
- [31] L. A. Correa, M. Mehboudi, G. Adesso, and A. Sanpera, “Individual Quantum Probes for Optimal Thermometry,” *Phys. Rev. Lett.* **114**, 220405 (2015).
- [32] H.-P. Breuer, B. Kappler, and F. Petruccione, “The time-convolutionless projection operator technique in the quantum theory of dissipation and decoherence,” *Ann. Phys.* **291**, 36–70 (2001); H.-P. Breuer, J. Gemmer, and M. Michel, “Non-Markovian quantum dynamics: Correlated projection superoperators and Hilbert space averaging,” *Phys. Rev. E* **73**, 016139 (2006).
- [33] A. Uhlmann, “The “transition probability” in the state space of a-algebra,” *Rep. Math. Phys.* **9**, 273–279 (1976).
- [34] R. Jozsa, “Fidelity for mixed quantum states,” *J. Mod. Opt.* **41**, 2315–2323 (1994).
- [35] A. Uhlmann, “The metric of Bures and the geometric phase,” in *Groups and related Topics* (Springer, 1992) pp. 267–274.
- [36] M. A. Nielsen and I. L. Chuang, *Quantum Computation and Quantum Information* (Cambridge University Press, Cambridge, England, 2010).
- [37] A. Einstein, “Die plancksche theorie der strahlung und die theorie der spezifischen wärme,” *Ann. Phys. (Berlin)* **327**, 180–190 (1906).
- [38] U. Weiss, *Quantum dissipative systems*, Vol. 13 (World Scientific Pub Co Inc, 2008).
- [39] Splitting the Hamiltonian into a potential and a kinetic term $H = U(x, x_\mu) + K(p, p_\mu)$, one can see that effective potential felt by the probe is given by $U(x, x_\mu^*)$, where $x_\mu^* = -\frac{g_\mu}{m_\mu \omega_\mu^2}$ [i.e. $\partial_{x_\mu} U = 0$ at x_μ^*]. This is $U(x, x_\mu^*) = \frac{1}{2}(\omega_0^2 - \omega_R^2)x^2$. As a result, the high temperature limit of the reduced steady state of the probe obtained from the bare model $H = H_p + H_s + H_{p-s}$ is $\text{tr}_s \rho \propto \exp\left(-\frac{1}{2T}(\omega^2 - \omega_R^2)x^2 - \frac{1}{2T}p^2\right)$, which may differ significantly from the corresponding thermal state $\rho_T = Z^{-1} \exp(-H_p/T)$ if the couplings g_μ are strong. To correct this, one must introduce the frequency shift ω_R^2 in H_p *ad hoc*.
- [40] The need to introduce the cutoff frequency ω_c is related to the fact that even if very large (as compared to the probe), the sample is finite and thus, it has a maximum energy. The nonequilibrium steady state of the central oscillator will unavoidably depend on the choice of ω_c but, as long as $\omega_c \gg \omega_0$, this dependence should be weak and not change its qualitative features [42]. In particular, note that $\omega_R^2 \equiv \frac{2}{\pi} \int_0^\infty d\omega \frac{J(\omega)}{\omega} = 2\gamma\omega_c$.
- [41] H. Grabert, U. Weiss, and P. Talkner, “Quantum theory of the damped harmonic oscillator,” *Z. Phys. B* **55**, 87–94 (1984).
- [42] L. A. Correa, A. A. Valido, and D. Alonso, “Asymptotic discord and entanglement of nonresonant harmonic oscillators under weak and strong dissipation,” *Phys. Rev. A* **86**, 012110 (2012).

- [43] A. A. Valido, L. A. Correa, and D. Alonso, “Gaussian tripartite entanglement out of equilibrium,” *Phys. Rev. A* **88**, 012309 (2013); A. A. Valido, D. Alonso, and S. Kohler, “Gaussian entanglement induced by an extended thermal environment,” *Phys. Rev. A* **88**, 042303 (2013); A. A. Valido, A. Ruiz, and D. Alonso, “Quantum correlations and energy currents across three dissipative oscillators,” *Phys. Rev. E* **91**, 062123 (2015).
- [44] A. Ferraro, S. Olivares, and M. G. A. Paris, *Gaussian states in continuous variable quantum information* (Bibliopolis, Napoli, 2005).
- [45] H. Scutaru, “Fidelity for displaced squeezed thermal states and the oscillator semigroup,” *J. Phys. A: Math. Gen.* **31**, 3659 (1998).
- [46] A. Monras, “Phase space formalism for quantum estimation of Gaussian states,” *arXiv preprint arXiv:1303.3682* (2013).
- [47] T. Bastin, J. von Zanthier, and E. Solano, “Measurement of phonon-number moments and motional quadratures through infinitesimal-time probing of trapped ions,” *J. Phys. B: At. Mol. Opt. Phys.* **39**, 685 (2006).
- [48] C. D’Helon and G. J. Milburn, “Reconstructing the vibrational state of a trapped ion,” *Phys. Rev. A* **54**, R25–R28 (1996).
- [49] J. F. Poyatos, R. Walser, J. I. Cirac, P. Zoller, and R. Blatt, “Motion tomography of a single trapped ion,” *Phys. Rev. A* **53**, R1966–R1969 (1996).
- [50] A. G. Kofman, G. Kurizki, and B. Sherman, “Spontaneous and induced atomic decay in photonic band structures,” *J. Mod. Opt.* **41**, 353–384 (1994).
- [51] J. F. Poyatos, J. I. Cirac, and P. Zoller, “Quantum Reservoir Engineering with Laser Cooled Trapped Ions,” *Phys. Rev. Lett.* **77**, 4728–4731 (1996).
- [52] A. Zwick, G. A. Álvarez, and G. Kurizki, “Maximizing Information on the Environment by Dynamically Controlled Qubit Probes,” *Phys. Rev. Applied* **5**, 014007 (2016).
- [53] A. García-Saez, A. Ferraro, and A. Acín, “Local temperature in quantum thermal states,” *Phys. Rev. A* **79**, 052340 (2009).
- [54] Elliott Lieb, Theodore Schultz, and Daniel Mattis, “Two soluble models of an antiferromagnetic chain,” *Annals of Physics* **16**, 407–466 (1961).
- [55] S. Sachdev, *Quantum Phase Transitions* (Cambridge University Press, Cambridge, England, 2011).
- [56] D. Reeb and M. M. Wolf, “Tight Bound on Relative Entropy by Entropy Difference,” *IEEE Trans. Inf. Theory* **61**, 1458–1473 (2015).
- [57] M. Cramer and J. Eisert, “Correlations, spectral gap and entanglement in harmonic quantum systems on generic lattices,” *New J. Phys.* **8**, 71 (2006).
- [58] G. De Palma, A. De Pasquale, and V. Giovannetti, “Universal locality of quantum thermal susceptibility,” *arXiv:1611.05738 [quant-ph]*.
- [59] H. Bateman, “Tables of integral transforms (vol. II),” California Institute of Technology Bateman Manuscript Project, New York: McGraw-Hill, 1954, edited by Erdelyi, Arthur **1** (1954).

SUPPLEMENTAL MATERIAL FOR “LOW-TEMPERATURE THERMOMETRY ENHANCED BY STRONG COUPLING”

Appendix A: Exponential suppression of local thermometry in systems with short-range interactions at low temperatures

In this section we prove that small parts of large many-body systems with short-range interactions become insensitive to the global temperature *exponentially* with the inverse of the temperature, irrespective of the strength of the interactions. The proof is instructive in the sense that it provides a heuristic argument as to why the main claim should hold in general.

We have in mind the following set-up: a translationally invariant lattice of identical systems (e.g. spins or oscillators) with short-range interactions and in global thermal equilibrium. Our aim is to do thermometry with a finite-size subsystem S of the lattice. We consider the lattice to be arbitrarily large and to be away from criticality.

Recall from Eq. (1) in the main text that the QFI for temperature estimation is $\mathcal{F}_T = -2 \lim_{\delta \rightarrow 0} \partial^2 \mathbb{F}(\rho_T, \rho_{T+\delta}) / \partial \delta^2$ (where ρ_T denotes the marginal of the subsystem S when the global many-body system is at temperature T). In what follows, it will be convenient to cast \mathcal{F}_T in the equivalent form

$$\mathcal{F}_T = 4 \lim_{\delta \rightarrow 0} \frac{1 - \mathbb{F}(\rho_T, \rho_{T+\delta})}{\delta^2}, \quad (\text{S1})$$

so that the Uhlmann fidelity between ρ_T and $\rho_{T+\delta}$ writes as

$$\mathbb{F}(\rho_T, \rho_{T+\delta}) = \left(\text{tr} \sqrt{\sqrt{\rho_T} \rho_{T+\delta} \sqrt{\rho_T}} \right)^2 = 1 - \frac{1}{4} \mathcal{F}_T \delta^2 + \mathcal{O}(\delta^3).$$

To see that this is indeed the case, let us denote $\rho_{T+\delta} = \rho_T + x$, where $x := \frac{\partial \rho_T}{\partial T} \delta + \mathcal{O}(\delta^2) = \mathcal{O}(\delta)$ and $\text{tr} x = 0$. Hence,

$$\sqrt{\mathbb{F}(\rho_T, \rho_{T+\delta})} = \text{tr} \sqrt{\sqrt{\rho_T} (\rho_T + x) \sqrt{\rho_T}} = \text{tr} \sqrt{\rho_T^2 + \sqrt{\rho_T} x \sqrt{\rho_T}}.$$

Next, let us introduce y as in $\sqrt{\rho_T^2 + \sqrt{\rho_T} x \sqrt{\rho_T}} = \rho_T + y$, so that, by taking the square on both sides, we get

$$y^2 + \rho_T y + y \rho_T = \sqrt{\rho_T} x \sqrt{\rho_T}. \quad (\text{S2})$$

From here it is obvious that $y = \mathcal{O}(\delta)$ as well. Let us now multiply Eq. (S2) by $(\sqrt{\rho_T})^{-1}$ both from the left and from the right. Note that we can work exclusively on the support of ρ_T , and treat it as invertible, even if it is not full-rank, since we are interested in $\mathcal{O}(\delta)$ terms and everything in Eq. (S2) is multiplied by ρ_T , except for a term of $\mathcal{O}(\delta^2)$. We thus arrive at

$$\delta \frac{\partial \rho_T}{\partial T} + \mathcal{O}(\delta^2) = (\sqrt{\rho_T})^{-1} y \sqrt{\rho_T} + \sqrt{\rho_T} y (\sqrt{\rho_T})^{-1} + \mathcal{O}(\delta^2), \quad (\text{S3})$$

where in y/δ one immediately recognizes the symmetric logarithmic derivative \mathcal{L}_T , defined by $\partial \rho_T / \partial T = \frac{1}{2} \{\rho_T, \mathcal{L}_T\}$, through the relation $\lim_{\delta \rightarrow 0} y/\delta = \frac{1}{2} \rho_T^{1/2} \mathcal{L}_T \rho_T^{1/2}$. Now, taking the trace in Eq. (S3) and noticing that $\text{tr}(\partial \rho_T / \partial T) = \partial(\text{tr} \rho_T) / \partial T = 0$, and using the cyclicity of matrix product under trace, we get that $\text{tr} y = \mathcal{O}(\delta^2)$. Hence, we finally see that

$$\mathbb{F}(\rho_T, \rho_{T+\delta}) = 1 + \frac{1}{2} \left(\lim_{\delta \rightarrow 0} \frac{\partial^2 \mathbb{F}(\rho_T, \rho_{T+\delta})}{\partial \delta^2} \right) \delta^2 + \mathcal{O}(\delta^3) = 1 - \frac{1}{4} \mathcal{F}_T \delta^2 + \mathcal{O}(\delta^3), \quad (\text{S4})$$

which agrees with (S1). Note that $\mathcal{F}_T \geq 0$ because otherwise the fidelity would exceed 1. The expansion (S4) can also be seen as an expression of the fact that, as a function of δ , $\mathbb{F}(\rho_T, \rho_{T+\delta})$ has a global local maximum at $\delta = 0$.

Turning to the Bures metric, we first notice that $\sqrt{\mathbb{F}(\rho_T, \rho_{T+\delta})} = 1 - \frac{1}{8} \mathcal{F}_T \delta^2 + \mathcal{O}(\delta^3)$. Hence, recalling from the main text that the Bures distance is defined as $d_B^2(\rho_T, \rho_{T+\delta}) = 2 \left(1 - \sqrt{\mathbb{F}(\rho_T, \rho_{T+\delta})} \right)$, we may also write

$$d_B^2(\rho_T, \rho_{T+\delta}) = \frac{1}{4} \mathcal{F}_T \delta^2 + \mathcal{O}(\delta^3). \quad (\text{S5})$$

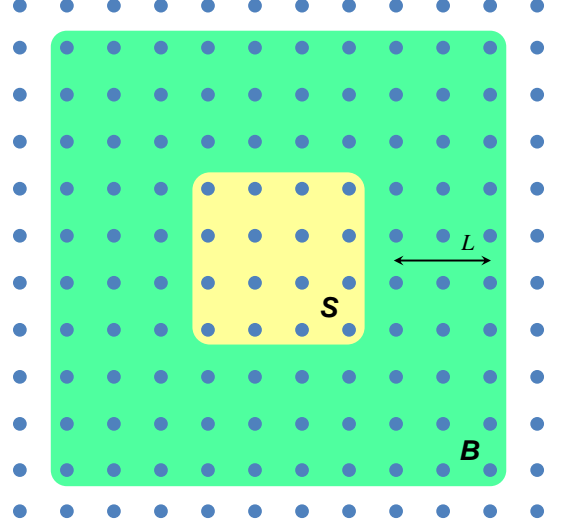


FIG. S1. Schematic image of the lattice, the system S , and the boundary B of length L (see text for details).

In addition to the system S of size L_S , we now bring the *boundary* B of size L into play (see Fig. S1). Let us introduce the thermal equilibrium state $\tau_T(L_S, L)$ on the composite ‘system + boundary’. We will denote the corresponding system marginal by $\rho_T(L) := \text{tr}_B \tau_T(L_S, L)$. In the limit of large boundary, we recover the original local state of S (i.e. $\rho_T(\infty) = \rho_T$).

With this notation in mind, from the triangle inequality for Bures distance it follows that

$$d_B(\rho_T, \rho_{T+\delta}) \leq d_B(\rho_T(L), \rho_{T+\delta}(L)) + d_B(\rho_T, \rho_T(L)) + d_B(\rho_{T+\delta}, \rho_{T+\delta}(L)). \quad (\text{S6})$$

We can now use the data-processing inequality for Bures distance [36] in the first term of (S6) to obtain $d_B(\rho_T(L), \rho_{T+\delta}(L)) \leq d_B(\tau_T(L_S, L), \tau_{T+\delta}(L_S, L))$. Furthermore, recalling that for thermal states the Fisher information is related to the heat capacity through $\mathcal{F}_T = C(T)/T^2$, and using (S5), we get that $d_B(\tau_T(L_S, L), \tau_{T+\delta}(L_S, L)) = \frac{\sqrt{C_{S+B}(T)}}{2T} \delta + \mathcal{O}(\delta^2)$. This yields

$$d_B(\rho_T, \rho_{T+\delta}) \leq \frac{\sqrt{C_{S+B}(T)}}{2T} \delta + \mathcal{O}(\delta^2) + d_B(\rho_T, \rho_T(L)) + d_B(\rho_{T+\delta}, \rho_{T+\delta}(L)). \quad (\text{S7})$$

Next, we are going to use the results of [18, 19, 53] about approximating $\rho_T = \rho_T(\infty)$ by $\rho_T(L)$ for finite L . Although the results in [18, 19] – and hence in this appendix as well – apply to rather general systems, in what follows, for simplicity, we will focus on the quantum Ising model in a transverse field [54]. Namely,

$$H_I = \frac{1}{2} \sum_i \sigma_x^i \otimes \sigma_x^{i+1} - \frac{h}{2} \sum_i \sigma_z^i. \quad (\text{S8})$$

Away from criticality ($h \neq 1$) and for large L , one finds that

$$\mathbb{F}(\rho_T(L), \rho_T) = 1 - \mathcal{O}(1)e^{-L/\xi(T,h)}, \quad (\text{S9})$$

where $\xi(T, h)$ is a monotonic function of the correlation length of the infinite chain and a regular function of T , even when $T \rightarrow 0$ (again, $h \neq 1$) [55]. We then have

$$d_B(\rho_T(L), \rho_T) = \mathcal{O}(1)e^{-\frac{L}{2\xi(T,h)}}. \quad (\text{S10})$$

In order to bound (S7), we will introduce the notation $\xi := \max\{\xi(T, h), \xi(T + \delta, h)\}$, and rewrite (S7) as

$$d_B(\rho_T, \rho_{T+\delta}) \leq \frac{\sqrt{C_{S+B}(T)}}{2T} \delta + \mathcal{O}(\delta^2) + \mathcal{O}(1)e^{-\frac{L}{2\xi}}. \quad (\text{S11})$$

Let us now turn to the heat capacity $C_{S+B}(T)$ of the ‘system + boundary’, which comprises $L_S + L$ spins. In the free-fermion representation [55], $H_I = \sum_{k=1}^{L_S+L} \varepsilon_k (c_k^\dagger c_k - 1/2)$, where c_k and c_k^\dagger are the annihilation and creation operators of the k -th fermionic mode, and $\varepsilon_k = 2\sqrt{1 + h^2 - 2h \cos\left(\frac{2\pi k}{L_S+L}\right)}$, for $k \in \{-\lfloor \frac{L_S+L}{2} \rfloor, \dots, \lfloor \frac{L_S+L}{2} \rfloor - 1\}$. In other words, the spin chain may be effectively described by $L_S + L$ non-interacting two-level systems with different energy gaps. The smallest gap is lower-bounded by (and approximately equal to) $\Delta = |h - 1|$. Therefore,

$$C_{S+B}(T) \leq (L_S + L)C(\Delta, T), \quad (\text{S12})$$

where $C(\Delta, T)$ is the heat capacity of a two-level system with gap Δ , at temperature T :

$$C(\Delta, T) = \frac{(\beta\Delta)^2 e^{-\beta\Delta}}{(1 + e^{-\beta\Delta})^2}. \quad (\text{S13})$$

Substituting (S12) and (S13) in (S11), we obtain

$$d_B(\rho_T, \rho_{T+\delta}) \leq \mathcal{O}(1) \left[\sqrt{L_S + L} (\beta\Delta)^2 e^{-\frac{\beta\Delta}{2}} \delta + e^{-\frac{L}{2\xi}} + \delta^2 \right]. \quad (\text{S14})$$

Now, since we are interested in the low-temperature regime, we want to know the behaviour of $d_B(\rho_T, \rho_{T+\delta})$ in the $\beta \rightarrow \infty$ limit. Therefore, the foremost thing is to make sure that δ is much smaller than T (so that our Taylor expansions above make sense). To guarantee that, let us choose

$$\delta = e^{-\beta\Delta} \quad (\text{which is } \ll (\beta\Delta)^{-1} \text{ for } \beta\Delta \gg 1), \quad (\text{S15})$$

where we multiply β by Δ (a fixed quantity) for dimension-neutralization purposes only. Furthermore, let us choose

$$L = 4\xi\beta\Delta \quad (\gg 1 \text{ for } \beta\Delta \gg 1, \text{ as needed}). \quad (\text{S16})$$

Finally, substituting (S15) and (S16) into (S14), we arrive at

$$d_B(\rho_T, \rho_{T+\delta}) \leq \mathcal{O}(1) \left[(\beta\Delta)^2 \sqrt{\beta\Delta} e^{-\frac{3}{2}\beta\Delta} + 2e^{-2\beta\Delta} \right] = \mathcal{O}(1) (\beta\Delta)^{\frac{5}{2}} e^{-\frac{3}{2}\beta\Delta}, \quad (\text{S17})$$

which leads to Eq. (2) in the main text when combined with (S5) and (S15); that is

$$\mathcal{F}_T \leq \mathcal{O}(1) (\beta\Delta)^5 e^{-\beta\Delta} \quad \text{for } \beta\Delta \gg 1. \quad (\text{S18})$$

Inequality (S18) is rather general and goes well beyond the quantum Ising model. Indeed, Eq. (S7) is valid in the most general case. Up to irrelevant (to the present problem) changes in the $\mathcal{O}(1)$ prefactor, Eq. (S9) generically holds for locally finite short-range interacting systems away from criticality [18, 19]. Next, the scaling of Eqs. (S12) and (S14) is also generic to locally finite systems with short-range interactions. This can easily be seen by noticing that with the increasing size of the boundary, the system plus boundary Hamiltonian's gap approaches the gap Δ of the infinite lattice, hence the heat capacity will scale like $e^{-\beta\Delta}$. On the other hand, we know that *system-size-wise*, the heat capacity scales at most like N^2 , where N is the number of lattice sites in system plus boundary (like $L_S + L$ above) [56]. Hence, the overall scaling will be $C(T) \sim N^2 e^{-\beta\Delta}$. This gives the last of the necessary ingredients for proving Eq. (S18) in the general case. Notice, however, that the degree of the polynomial prefactor in (S18) will in general be different and depend on both the spatial dimensionality of the lattice and whether the heat capacity is extensive or super-extensive. For example, in the worst case scenario, namely, when the lattice is three-dimensional with its heat capacity scaling as N^2 , the prefactor will be $(\beta\Delta)^{10}$.

One can very easily go even further and prove such an inequality also for harmonic lattices. Indeed, given the results in [17] about approximating $\rho_T(\infty)$ with $\rho_T(L)$ and the results in [57] about the relation between the spectral gap and exponential decay of correlations in harmonic lattices, the analysis is identical to the quantum Ising case, especially when taking into account that, although the results of [56] for the heat capacity do not apply here, the 'system + boundary' Hamiltonian can again be decomposed in $\propto N$ harmonic modes, each of which has a finite heat capacity that scales like $e^{-\beta\omega}$ with $\beta \gg 1$, where ω is the frequency of each mode.

All in all, Eq. (S18) shows that local thermometry is exponentially inefficient at low temperatures, and is generic to arbitrarily strongly but short-range interacting lattices, irrespective of their spatial dimension or their being fermionic or bosonic. Moreover, provided the generalized correlations (see [18] for the definition) decay exponentially, the translation-invariance of the lattice can also be abandoned [18]. This motivates us to propose practical enhanced low-temperature thermometric strategies capable of rendering the best attainable precision, given the stringent fundamental limitations in force.

As a final remark, let us note that, in accounting for the boundary effects arising due to the interactions, the analysis in this appendix is similar in spirit to Refs. [25, 58]. They differ, however, in the precise questions addressed and the results obtained.

Appendix B: From the Heisenberg equations of motion to the QLE

We can write down the Heisenberg equations of motion $\left(\frac{d}{dt} A(t) = i[H, A(t)] + \partial_t A(t) \right)$ for all degrees of freedom $\{x, p, x_\mu, p_\mu\}$ of the system $H = H_p + H_s + H_{p-s}$. These read

$$\dot{x} = p \quad (\text{S1a})$$

$$\dot{p} = -\left(\omega_0^2 + \omega_R^2 \right) x - \sum_\mu g_\mu x_\mu \quad (\text{S1b})$$

$$\dot{x}_\mu = \frac{p_\mu}{m_\mu} \quad (\text{S1c})$$

$$\dot{p}_\mu = -m_\mu \omega_\mu^2 x_\mu - g_\mu x. \quad (\text{S1d})$$

Differentiating Eq. (S1c) and inserting in it Eq. (S1d) yields $\ddot{x}_\mu + \omega_\mu^2 x_\mu = -\frac{g_\mu}{m_\mu} x$, which results in

$$x_\mu(t) = x_\mu(t_0) \cos \omega_\mu(t-t_0) + \frac{p_\mu(t_0)}{m_\mu \omega_\mu} \sin \omega_\mu(t-t_0) - \frac{g_\mu}{m_\mu \omega_\mu} \int_{t_0}^t ds \sin \omega_\mu(t-s) x(s). \quad (\text{S2})$$

Similarly, one can differentiate Eq. (S1a) and use Eqs. (S1b) and (S2) to eliminate \dot{p} and x_μ . This results in the following integro-differential equation

$$\ddot{x} + \left(\omega_0^2 + \omega_R^2 \right) x - \int_{t_0}^t ds \sum_\mu \frac{g_\mu^2}{m_\mu \omega_\mu} \sin \omega_\mu(t-s) x(s) = - \sum_\mu g_\mu \left(x_\mu(t_0) \cos \omega_\mu(t-t_0) + \frac{p_\mu(t_0)}{m_\mu \omega_\mu} \sin \omega_\mu(t-t_0) \right). \quad (\text{S3})$$

This is nothing but the quantum Langevin equation (QLE) of our system. Since we are interested in the steady state of the central oscillator, we may let $t_0 \rightarrow -\infty$ without loss of generality. Defining the stochastic quantum force

$$F(t) := -\sum_{\mu} g_{\mu} \left(x_{\mu}(t_0) \cos \omega_{\mu}(t-t_0) + \frac{p_{\mu}(t_0)}{m_{\mu} \omega_{\mu}} \sin \omega_{\mu}(t-t_0) \right), \quad (\text{S4})$$

and the dissipation kernel

$$\chi(t) := \sum_{\mu} \frac{g_{\mu}^2}{m_{\mu} \omega_{\mu}} \sin \omega_{\mu} t \Theta(t) = \frac{2}{\pi} \int_0^{\infty} d\omega J(\omega) \sin \omega t \Theta(t), \quad (\text{S5})$$

one may rewrite the QLE as

$$\ddot{x}(t) + \left(\omega_0^2 + \omega_R^2 \right) x(t) - x(t) * \chi(t) = F(t), \quad (\text{S6})$$

where $*$ denotes convolution.

Appendix C: Solving the QLE for the steady state of the central oscillator

As explained in the main text, any Gaussian state (such as the steady state of the probe) is fully characterized by its first and second-order moments. In the case of a single-mode Gaussian state, these latter can be arranged in the 2×2 real and symmetric covariance matrix σ . We therefore must be able to compute objects like $\langle \{x(t'), x(t'')\} \rangle$, $\langle \{p(t'), p(t'')\} \rangle$ and $\langle \{x(t'), p(t'')\} \rangle$ from Eq. (S6). Let us start by taking its Fourier transform, which gives

$$-\omega^2 \tilde{x} + (\omega_0^2 + \omega_R^2) \tilde{x} + \tilde{x} \tilde{\chi} = \tilde{F} \Rightarrow \tilde{x}(\omega) = \frac{\tilde{F}(\omega)}{\omega_0^2 + \omega_R^2 - \omega^2 - \tilde{\chi}(\omega)} := \alpha(\omega)^{-1} \tilde{F}(\omega). \quad (\text{S1})$$

Note that

$$\begin{aligned} \frac{1}{2} \langle \{x(t'), x(t'')\} \rangle &= \frac{1}{2} \int_{-\infty}^{\infty} \frac{d\omega'}{2\pi} e^{-i\omega't'} \int_{-\infty}^{\infty} \frac{d\omega''}{2\pi} e^{-i\omega''t''} \langle \{ \tilde{x}(\omega'), \tilde{x}(\omega'') \} \rangle \\ &= \frac{1}{2} \int_{-\infty}^{\infty} \frac{d\omega'}{2\pi} e^{-i\omega't'} \int_{-\infty}^{\infty} \frac{d\omega''}{2\pi} e^{-i\omega''t''} \alpha(\omega')^{-1} \alpha(\omega'')^{-1} \langle \{ \tilde{F}(\omega'), \tilde{F}(\omega'') \} \rangle_T. \end{aligned} \quad (\text{S2})$$

Therefore, all what is left is to find the analytical expression of the power spectrum of the bath $2^{-1} \langle \{ \tilde{F}(\omega'), \tilde{F}(\omega'') \} \rangle_T$ and of the Fourier transform of the susceptibility $\tilde{\chi}(\omega)$, which appears in $\alpha(\omega)$. Note that the Fourier transform of all first order moments will be proportional to $\langle \tilde{F}(\omega) \rangle_T$ which is identically zero [cf. Eq. (S4)]. Hence, the steady states of the central oscillator will be *undisplaced* Gaussians. With the subscript in $\langle \dots \rangle_T$, we emphasize that the average is taken over the initial Gibbs state of the sample.

1. The fluctuation-dissipation relation

Let us start by computing $\frac{1}{2} \langle \{ \tilde{F}(\omega'), \tilde{F}(\omega'') \} \rangle_T = \text{Re} \langle \tilde{F}(\omega') \tilde{F}(\omega'') \rangle_T$ from Eq. (S4). Taking into account that $\langle x_{\mu}(t_0) x'_{\mu}(t_0) \rangle_T = \delta_{\mu\mu'} (2m_{\mu} \omega_{\mu})^{-1} [1 + 2n_{\mu}(T)]$, $\langle p_{\mu}(t_0) p'_{\mu}(t_0) \rangle_T = \delta_{\mu\mu'} \frac{1}{2} m_{\mu} \omega_{\mu} [1 + 2n_{\mu}(T)]$ and $\langle x_{\mu}(t_0) p_{\mu}(t_0) \rangle_T = \langle p_{\mu}(t_0) x_{\mu}(t_0) \rangle_T^* = i/2$, one has

$$\begin{aligned} \frac{1}{2} \langle \{ \tilde{F}(t'), \tilde{F}(t'') \} \rangle_T &= \frac{1}{\pi} \sum_{\mu} \frac{\pi g_{\mu}^2}{2m_{\mu} \omega_{\mu}} [1 + 2n_{\mu}(T)] [\cos \omega_{\mu}(t' - t_0) \cos \omega_{\mu}(t'' - t_0) + \sin \omega_{\mu}(t' - t_0) \sin \omega_{\mu}(t'' - t_0)] \\ &= \frac{1}{\pi} \int_0^{\infty} d\omega J(\omega) \coth \frac{\omega}{2T} \cos \omega(t' - t''), \end{aligned} \quad (\text{S3})$$

where we have used $2n_\mu(T) + 1 = \coth(\omega_\mu/2T)$, which follows from the definition of the bosonic thermal occupation number $n_\mu(T) \equiv [\exp(\omega/2T) - 1]^{-1}$. Now, taking the Fourier transform of Eq. (S3) yields

$$\begin{aligned}
\frac{1}{2} \langle \{\tilde{F}(\omega'), \tilde{F}(\omega'')\} \rangle_T &= 2\pi \int_{-\infty}^{\infty} \frac{dt'}{2\pi} e^{i\omega't'} \int_{-\infty}^{\infty} \frac{dt''}{2\pi} e^{i\omega''t''} \int_0^{\infty} d\omega J(\omega) \coth \frac{\omega}{2T} \left(e^{i\omega(t'-t'')} + e^{-i\omega(t'-t'')} \right) \\
&= 2\pi \int_{-\infty}^{\infty} \frac{dt'}{2\pi} \int_{-\infty}^{\infty} \frac{dt''}{2\pi} \int_0^{\infty} d\omega J(\omega) \coth \frac{\omega}{2\pi} \left(e^{it'(\omega+\omega')} e^{it''(\omega''-\omega)} + e^{it'(\omega'-\omega)} e^{it''(\omega''+\omega)} \right) \\
&= 2\pi \int_0^{\infty} d\omega J(\omega) \coth \frac{\omega}{2T} \left[\delta(\omega + \omega') \delta(\omega'' - \omega) + \delta(\omega' - \omega) \delta(\omega'' + \omega) \right] \\
&= 2\pi \delta(\omega' + \omega'') \coth \frac{\omega'}{2T} \left[J(\omega') \Theta(\omega') - J(-\omega') \Theta(-\omega') \right], \quad (\text{S4})
\end{aligned}$$

where we have used the identity $\int_{-\infty}^{\infty} dt e^{i\omega t} = 2\pi \delta(\omega)$. On the other hand, we may find $\text{Im} \tilde{\chi}(\omega)$ from Eq. (S5). Note that

$$\begin{aligned}
\text{Im} \tilde{\chi}(\omega) &= \text{Im} \sum_{\mu} \frac{g_{\mu}^2}{m_{\mu} \omega_{\mu}} \int_{-\infty}^{\infty} dt e^{i\omega t} \Theta(t) \sin \omega_{\mu} t = \sum_{\mu} \frac{g_{\mu}^2}{m_{\mu} \omega_{\mu}} \int_0^{\infty} dt \sin \omega t \sin \omega_{\mu} t \\
&= \frac{1}{4} \sum_{\mu} \frac{g_{\mu}^2}{m_{\mu} \omega_{\mu}} \int_0^{\infty} dt \left[e^{i(\omega+\omega_{\mu})t} - e^{i(\omega-\omega_{\mu})t} - e^{i(-\omega+\omega_{\mu})t} + e^{-i(\omega+\omega_{\mu})t} \right] = \frac{1}{4} \sum_{\mu} \frac{g_{\mu}^2}{m_{\mu} \omega_{\mu}} \left(\int_{-\infty}^{\infty} dt e^{i(\omega+\omega_{\mu})t} - \int_{-\infty}^{\infty} dt e^{i(\omega-\omega_{\mu})t} \right) \\
&= \frac{\pi}{2} \sum_{\mu} \frac{g_{\mu}^2}{m_{\mu} \omega_{\mu}} \left[\delta(\omega - \omega_{\mu}) - \delta(\omega + \omega_{\mu}) \right] = \int_0^{\infty} d\omega J(\omega) \left[\delta(\omega - \omega_{\mu}) - \delta(\omega + \omega_{\mu}) \right] \\
&= J(\omega) \Theta(\omega) - J(-\omega) \Theta(-\omega). \quad (\text{S5})
\end{aligned}$$

Hence the fluctuation-dissipation relation $\langle \{\tilde{F}(t'), \tilde{F}(t'')\} \rangle = 4\pi \delta(\omega' + \omega'') \coth(\omega'/2T) \text{Im} \tilde{\chi}(\omega')$. When it comes to its real part, the calculation is not so straightforward. Recall from Eq. (S5) that the response function $\chi(t)$ is *causal* due to the accompanying Heaviside step function. Causal response functions have analytic Fourier transform in the upper-half of the complex plane and therefore, the Kramers-Kronig relations hold [38]. In particular

$$\text{Re} \tilde{\chi}(\omega) = \frac{1}{\pi} \text{P} \int_{-\infty}^{\infty} d\omega' \frac{\text{Im} \tilde{\chi}(\omega')}{\omega' - \omega} \equiv \mathcal{H} \text{Im} \tilde{\chi}(\omega), \quad (\text{S6})$$

where we have introduced the Hilbert transform $g(y) = \mathcal{H} f(x) := \pi^{-1} \text{P} \int_{-\infty}^{\infty} dx f(x)/(x-y)$ [59], and P denotes Cauchy principal value.

Appendix D: Dissipation kernel for Ohmic and super-Ohmic spectral densities with exponential cutoff

We will now obtain $\text{Re} \tilde{\chi}(\omega)$ for two instances of the family of spectral densities $J_s(\omega) := \frac{\pi}{2} \gamma \omega^s \omega_c^{1-s} e^{-\omega/\omega_c}$, namely $s = 1$ (Ohmic case) and $s = 2$ (super-Ohmic case). To begin with, let us list four useful properties of the Hilbert transform that we shall use in what follows

$$f(-ax) \xrightarrow{\mathcal{H}} -g(-ay) \quad a > 0 \quad (\text{S1a})$$

$$xf(x) \xrightarrow{\mathcal{H}} yg(y) + \frac{1}{\pi} \int_{-\infty}^{\infty} dx f(x) \quad (\text{S1b})$$

$$\exp(-a|x|) \xrightarrow{\mathcal{H}} \frac{1}{\pi} \text{sign} y \left[\exp(a|y|) \text{Ei}(-a|y|) - \exp(-a|y|) \overline{\text{Ei}}(a|y|) \right] \quad a > 0 \quad (\text{S1c})$$

$$\text{sign} x \exp(-a|x|) \xrightarrow{\mathcal{H}} -\frac{1}{\pi} \left[\exp(a|y|) \text{Ei}(-a|y|) + \exp(-a|y|) \overline{\text{Ei}}(a|y|) \right] \quad a > 0, \quad (\text{S1d})$$

where $\text{Ei}(x) \equiv -\int_{-x}^{\infty} dt t^{-1} e^{-t}$ is the exponential integral, and $\overline{\text{Ei}}(x)$ denotes its principal value.

a. Ohmic case ($s = 1$)

According to Eqs. (S6) and (S5), one has

$$\text{Re } \tilde{\chi}(\omega) = \frac{\pi\gamma}{2} \left\{ \mathcal{H}[\Theta(\omega') \omega' \exp(-\omega'/\omega_c)](\omega) - \mathcal{H}[-\Theta(-\omega') \omega' \exp(\omega'/\omega_c)](\omega) \right\}. \quad (\text{S2})$$

Using Eqs. (S1a) and (S1b), this rewrites as

$$\begin{aligned} \text{Re } \tilde{\chi}(\omega) &= \frac{\pi\gamma}{2} \left\{ \mathcal{H}[\Theta(\omega') \omega' \exp(-\omega'/\omega_c)](\omega) + \mathcal{H}[\Theta(\omega') \omega' \exp(-\omega'/\omega_c)](-\omega) \right\} \\ &= \frac{\pi\gamma}{2} \left\{ \omega \mathcal{H}[\Theta(\omega') \exp(-\omega'/\omega_c)](\omega) - \omega \mathcal{H}[\Theta(\omega') \exp(-\omega'/\omega_c)](-\omega) + \frac{2\omega_c}{\pi} \right\}. \end{aligned} \quad (\text{S3})$$

Now, using first Eq. (S1a) again, and then Eq. (S1c), one finds

$$\text{Re } \tilde{\chi}(\omega) = \gamma\omega_c + \frac{\pi\gamma}{2} \omega \mathcal{H}[\exp(-|\omega|/\omega_c)](\omega) = \gamma\omega_c - \frac{\gamma}{2} \omega \left[\exp(-\omega/\omega_c) \bar{\text{Ei}}(\omega/\omega_c) - \exp(\omega/\omega_c) \text{Ei}(-\omega/\omega_c) \right], \quad (\text{S4})$$

which can also be expressed in terms of the incomplete Euler's Gamma function $\Gamma(0, x) = -\text{Ei}(-x)$.

b. Super-Ohmic case ($s = 2$)

Using the properties of Eq. (S1) it is also straightforward to obtain $\text{Re } \tilde{\chi}(\omega)$ in the case of $s = 2$:

$$\begin{aligned} \text{Re } \tilde{\chi}(\omega) &= \frac{\pi\gamma}{2\omega_c} \left\{ \mathcal{H}[\Theta(\omega') \omega'^2 \exp(-\omega'/\omega_c)](\omega) - \mathcal{H}[\Theta(-\omega') \omega'^2 \exp(\omega'/\omega_c)](\omega) \right\} \\ &= \frac{\pi\gamma}{2\omega_c} \left\{ \mathcal{H}[\Theta(\omega') \omega'^2 \exp(-\omega'/\omega_c)](\omega) + \mathcal{H}[\Theta(\omega') \omega'^2 \exp(-\omega'/\omega_c)](-\omega) \right\} \\ &= \frac{\pi\gamma}{2\omega_c} \left\{ \omega \mathcal{H}[\Theta(\omega') \omega' \exp(-\omega'/\omega_c)](\omega) - \omega \mathcal{H}[\Theta(\omega') \omega' \exp(-\omega'/\omega_c)](-\omega) + \frac{2\omega_c^2}{\pi} \right\} \\ &= \gamma\omega_c + \frac{\pi\gamma}{2\omega_c} \left\{ \omega^2 \mathcal{H}[\Theta(\omega') \exp(-\omega'/\omega_c)](\omega) + \omega^2 \mathcal{H}[\Theta(\omega') \exp(-\omega'/\omega_c)](-\omega) \right\} \\ &= \gamma\omega_c + \frac{\pi\gamma}{2\omega_c} \omega^2 \mathcal{H}[\text{sign } \omega \exp(-|\omega|/\omega_c)](\omega) \\ &= \gamma\omega_c - \frac{\gamma}{2\omega_c} \omega^2 \left[\exp(-\omega/\omega_c) \bar{\text{Ei}}(\omega/\omega_c) + \exp(\omega/\omega_c) \text{Ei}(-\omega/\omega_c) \right]. \end{aligned} \quad (\text{S5})$$

Appendix E: Calculation of the steady-state covariances

Now we have all the ingredients to compute the steady-state covariances of the central oscillator. Note that

$$\frac{1}{2} \langle \{x(t'), x(t'')\} \rangle = \frac{1}{2} \int_{-\infty}^{\infty} \frac{d\omega'}{2\pi} e^{-i\omega't'} \int_{-\infty}^{\infty} \frac{d\omega''}{2\pi} e^{-i\omega''t''} \alpha(\omega')^{-1} \alpha(\omega'')^{-1} \langle \{ \tilde{F}(\omega'), \tilde{F}(\omega'') \} \rangle_T \quad (\text{S1})$$

$$= \int_{-\infty}^{\infty} \frac{d\omega'}{2\pi} e^{-i\omega't'} \int_{-\infty}^{\infty} d\omega'' e^{-i\omega''t''} \alpha(\omega')^{-1} \alpha(\omega'')^{-1} [J(\omega')\Theta(\omega') - J(-\omega')\Theta(-\omega')] \coth \frac{\omega'}{2T} \delta(\omega' + \omega'') \text{Im } \tilde{\chi}(\omega') \quad (\text{S2})$$

$$= \int_{-\infty}^{\infty} \frac{d\omega'}{2\pi} e^{-i\omega'(t'-t'')} \alpha(\omega')^{-1} \alpha(-\omega')^{-1} [J(\omega')\Theta(\omega') - J(-\omega')\Theta(-\omega')] \coth \frac{\omega'}{2T} \text{Im } \tilde{\chi}(\omega'). \quad (\text{S3})$$

This gives a closed expression for the position-position covariance. Note that, since $\tilde{p}(\omega) = -i\omega\tilde{x}(\omega)$, one has $2^{-1} \langle \{ \tilde{p}(\omega'), \tilde{x}(\omega'') \} \rangle = 0$ and

$$\frac{1}{2} \langle \{p(t'), p(t'')\} \rangle = \int_{-\infty}^{\infty} \frac{d\omega'}{2\pi} e^{-i\omega'(t'-t'')} \omega'^2 \alpha(\omega')^{-1} \alpha(-\omega')^{-1} [J(\omega')\Theta(\omega') - J(-\omega')\Theta(-\omega')] \coth \frac{\omega'}{2T} \text{Im } \tilde{\chi}(\omega'). \quad (\text{S4})$$

Therefore, we have fully characterized the steady state of a single harmonic oscillator in a bosonic bath. Note that the *only* underlying assumption is that the environment was prepared in an equilibrium state at temperature T . Specifically, this was required when evaluating the correlators $\langle \{x_\mu(t_0), x_\mu(t_0)\} \rangle_T$ and $\langle \{p_\mu(t_0), p_\mu(t_0)\} \rangle_T$ in Eq. (S3). Otherwise, our calculation is *completely general*. For a non-equilibrium bath, one would only need to recalculate Eqs. (S3) and (S4).

Appendix F: Dependence of the normal-mode frequencies on the coupling strength in a ‘star system’

Let us consider a finite *star system* with N modes. As already explained in the main text, this will be comprised of a central harmonic oscillator of bare frequency ω_0 (playing the role of the probe), dissipatively coupled to $N - 1$ independent peripheral oscillators with arbitrary frequencies $\omega_{\mu \in \{1, \dots, N-1\}}$ (representing the sample). We will choose linear probe-sample couplings of the form $x\gamma \sum_{\mu=1}^{N-1} g_\mu x_\mu$, where γ carries the order of magnitude of the coupling strengths. Note that we also allow for arbitrary frequency-distribution of the coupling constants g_μ .

Hence, the total N -particle Hamiltonian may be written as $\hat{H} = \frac{1}{2} \bar{x}^t \mathbb{V} \bar{x} + \frac{1}{2} |\bar{p}|^2$, with $\bar{x} = (x, x_1, \dots, x_{N-1})$ and $\bar{p} = (p, p_1, \dots, p_{N-1})$. For simplicity of notation, we will take unit mass for all particles. The $N \times N$ interaction matrix \mathbb{V} may thus be written as

$$\mathbb{V} = \gamma \begin{pmatrix} \gamma^{-1} \Omega_0^2 & g_1 & g_2 & \cdots & g_{N-2} & g_{N-1} \\ g_1 & \gamma^{-1} \omega_1^2 & 0 & \cdots & 0 & 0 \\ g_2 & 0 & \omega_2^2 & \cdots & 0 & 0 \\ \vdots & \vdots & \vdots & \ddots & \vdots & \vdots \\ g_{N-2} & 0 & 0 & \cdots & \gamma^{-1} \omega_{N-2}^2 & 0 \\ g_{N-1} & 0 & 0 & \cdots & 0 & \gamma^{-1} \omega_{N-1}^2 \end{pmatrix}. \quad (\text{S1})$$

The frequencies of the normal modes of the system are given by the square root of the N solutions λ_i of $P_N(\lambda_i) = |\mathbb{V} - \lambda_i \mathbb{1}| = 0$. Note that we have shifted the frequency of the central oscillator $\omega_0^2 \rightarrow \Omega_0^2 := \omega_0^2 + \sum_{\mu} g_\mu^2 / \omega_\mu^2$ to ensure that all $\lambda_i > 0$.

While it is hard to obtain closed expressions for λ_i , one may easily see the following: The frequencies of the modes above Ω_0 increase with the coupling strength, whereas those of the modes below Ω_0 decrease with γ (i.e. $\partial_\gamma \lambda_i > 0$ for $\lambda_i > \Omega_0^2$ and $\partial_\gamma \lambda_i < 0$ for $\lambda_i < \Omega_0^2$). Indeed, expanding $P_N(\lambda)$ by minors along the last row, yields the recurrence relation

$$P_N(\lambda) = (\omega_{N-1}^2 - \lambda) P_{N-1}(\lambda) - \gamma^2 g_{N-1}^2 \prod_{k=1}^{N-2} (\omega_k^2 - \lambda), \quad (\text{S2})$$

which allows to rewrite the condition $P_N(\lambda_i) = 0$ as

$$\Omega_0^2 - \lambda_i = \frac{1}{\prod_{l=1}^{N-1} \omega_l^2 - \lambda_i} \sum_{k=1}^{N-1} \gamma^2 g_k^2 \prod_{l=1}^{N-1} \frac{\omega_l^2 - \lambda_i}{\omega_k^2 - \lambda_i} = \sum_{k=1}^{N-1} \frac{\gamma^2 g_k^2}{\omega_k^2 - \lambda_i}. \quad (\text{S3})$$

Consequently, the derivative of any eigenvalue λ_i with respect to the coupling strength γ evaluates to

$$\partial_\gamma \lambda_i = - \frac{2\gamma \sum_{k=1}^{N-1} g_k^2 (\omega_k^2 - \lambda_i)^{-1}}{1 + \sum_{k=1}^{N-1} \gamma^2 g_k^2 (\omega_k^2 - \lambda_i)^{-2}}. \quad (\text{S4})$$

Comparing Eqs. (S3) and (S4) we can see that $\partial_\gamma \lambda_i > 0$ for $\lambda_i > \Omega_0^2$, and that, on the contrary, $\partial_\gamma \lambda_i < 0$ for $\lambda_i < \Omega_0^2$.